Modelling of impulse loading in high-temperature superconductors

Assessment of accuracy and performance of computational techniques

I.O. Golosnoy and J.K. Sykulski
Electrical Power Engineering Research Group, School of Electronics and Computer Science, University of Southampton, Southampton, UK

Abstract

Purpose – The aim of this paper is to access performance of existing computational techniques to model strongly non-linear field diffusion problems.

Design/methodology/approach – Multidimensional application of a finite volume front-fixing method to various front-type problems with moving boundaries and non-linear material properties is discussed. Advantages and implementation problems of the technique are highlighted by comparing the front-fixing method with computations using fixed grids. Particular attention is focused on conservation properties of the algorithm and accurate solutions close to the moving boundaries. The algorithm is tested using analytical solutions of diffusion problems with cylindrical symmetry with both spatial and temporal accuracy analysed.

Findings – Several advantages are identified in using a front-fixing method for modelling of impulse phenomena in high-temperature superconductors (HTS), namely high accuracy can be obtained with a small number of grid points, and standard numerical methods for convection problems with diffusion can be utilised. Approximately, first order of spatial accuracy is found for all methods (stationary or mobile grids) for 2D problems with impulse events. Nevertheless, errors resulting from a front-fixing technique are much smaller in comparison with fixed grids. Fractional steps method is proved to be an effective algorithm for solving the equations obtained. A symmetrisation procedure has to be introduced to eliminate a directional bias for a standard asymmetric split in diffusion processes.

Originality/value – This paper for the first time compares in detail advantages and implementation complications of a front-fixing method when applied to the front-type field diffusion problems common to HTS. Particular attention is paid to accurate solutions in the region close to the moving front where rapid changes in material properties are responsible for large computational errors.

Keywords Modelling, Numerical analysis, Diffusion, High temperatures, Superconductors

Paper type Research paper

1. Introduction

Using high-temperature superconductors (HTS) in modern devices not only promises significant energy savings, but also exposes difficulties in dealing with short circuit faults or other impulse loads. Such intensive impacts require coupled treatment of both electromagnetic and thermal parts of the problem since material properties of HTS are quite sensitive to temperature (Berger *et al.*, 2005). Standard numerical modelling of the pulse events on fixed grids provides valuable assistance in the equipment design but existing computational techniques not always provide appropriate balance between

COMPEL: The International Journal for Computation and Mathematics in Electrical and Electronic Engineering
Vol. 29 No. 4, 2010
pp. 1047-1059

0332-1649
DOI 10.1108/03321641011044460

accuracy and efficiency. More complex methods, such as adaptive meshes, front-fixing and level sets methods (Crank, 1984), offer advantages in applications to impulse problems but they have to be assessed and probably adapted for the particular problem. The paper uses analytical solutions of common front-type problems for the evaluation of the numerical methods. The main emphasis is on the analysis of the front-fixing technique (Crank, 1984), since it requires only a small adjustment of the computational algorithm in comparison with formulations using fixed grids (Golosnoy and Sykulski, 2008). Special attention is given to conservation properties of the algorithm and accurate solutions close to the moving boundaries.

2. Formulation of the problem

2.1 Governing equations

The problem of electric current flow in HTS can be formulated in terms of either magnetic or electric field diffusion (Rhyner, 1993; Sykulski *et al.*, 1997). The electric field formulation is preferred for HTS materials with highly non-linear properties since it provides much more stable solutions (Sykulski *et al.*, 1997). For this case, the governing equation takes the diffusion-like form:

$$\mathrm{curl}(\mathrm{curl}\ \mathbf{E}) = -\mu_0 \frac{\partial \mathbf{J}}{\partial t} \tag{1}$$

in terms of the electric field $\mathbf{E}$ and current density $\mathbf{J}$, but has to be supplemented by a relationship between field E and current density J. A strong flux creep E-J characteristic is a specific feature of HTS materials. This is often described by Rhyner's power law $E_c^{-1}E = (J_c^{-1}J)^{\alpha}$ (Rhyner, 1993), where the critical current density $J_c \approx 10^9\ \mathrm{A\,m^{-2}}$ corresponds to a critical electric field $E_c \approx 10^{-4}\ \mathrm{V\,m^{-1}}$ and a large power exponent α which for practical materials could be about 20. Substitution of the material properties into equation (1) results in a formulation of the problem in terms of the electric field only. It is worth noting that equation (1) can also be rewritten in terms of the electric current only:

$$\mathrm{curl}\left(\mathrm{curl}\left[\ \left(J_c^{-1}J\right)^{\alpha} E_c \hat{\mathbf{J}}\right]\ \right) = -\mu_0 \frac{\partial \mathbf{J}}{\partial t} \tag{2}$$

but the more commonly used expression is in terms of the electric field:

$$\mathrm{curl}(\mathrm{curl}\ \mathbf{E}) = -\mu_0 \frac{\partial\left[J_c\left(E_c^{-1}E\right)^{1/\alpha}\hat{\mathbf{E}}\right]}{\partial t} \tag{3}$$

Both equations (2) and (3) have advantages and disadvantages. The time derivative in equation (2) does not include the non-linear term and this makes an implementation of conservation laws more straightforward. On the other hand, the absolute variation in the non-linear term is smaller for equation (3) due to the $1/\alpha$ power. For this reason, equation (3) is less sensitive to rounding errors during calculations of impulse events.

2.2 Analytical solutions

It is helpful to conduct tests in at least 2D geometry. The existence of an analytical solution in cylindrical coordinates provides an opportunity to evaluate the technique's

performance on curved boundaries using the Cartesian coordinate system. Consider a HTS wire with a circular cross-section of radius R. If the current pulse:

$$J_z(r,t) = I_0\delta(\hat{\mathbf{r}})\delta(t-t_0) \tag{4}$$

is applied along the z-axis at instant $t = t_0$, the dimensionless solution for equation (1) in the case of cylindrical symmetry can be derived as shown in Pert (1977):

$$e(\rho,\tau) = \frac{1}{(\alpha\tau)}\left[\left(\frac{i_0}{4}\right)^{(\alpha-1)/\alpha} - \frac{\rho^2(\alpha-1)}{4\alpha(\alpha\tau)^{1/\alpha}}\right]^{\alpha/(\alpha-1)}, \quad e = i^{\alpha}, \tag{5}$$

with dimensionless length, time, electric field and current defined as:

$$\rho = \frac{r}{R}, \quad \tau = \frac{(t-t_0)E_c}{\mu_0 J_c R^2}, \quad i_0 = \frac{I_0}{J_c\pi R^2}, \quad e(\rho,\tau) = \frac{E_z(\rho,\tau)}{E_c}, \quad i(\rho,\tau) = \frac{J_z(\rho,\tau)}{J_c}. \tag{6}$$

Equation (5) is valid only inside $\rho \le \rho_b(\tau)$ and during limited time when $\rho_b(\tau) \le 1$ where:

$$\rho_b(\tau) = \left[\frac{4\alpha(\alpha\tau)^{1/\alpha}}{(\alpha-1)}\left(\frac{i_0}{4}\right)^{(\alpha-1)/\alpha}\right]^{1/2}. \tag{7}$$

The field and the current are zero outside the front region. The electric field and the current gradually spread from the centre of the wire towards the edges and there is a sharp interface between the region with non-zero field and the outside part of the wire. The field and current density profiles at different instances of time are shown at Figure 1.

2.3 Cartesian and cylindrical coordinates

Keeping in mind that the only non-zero component of electric field is in the z-direction, equation (3) for the cylinder takes the following form:

$$\frac{\partial}{\partial\tau}(\mathrm{sign}e\cdot|e|^{1/\alpha}) = \frac{1}{\rho}\frac{\partial}{\partial\rho}\left(\rho\frac{\partial e}{\partial\rho}\right), \quad \rho\in[0,1]. \tag{8}$$

The initial condition for equation (8) is:

$$i(\rho=0,\tau=0) = i_0\frac{\delta(\rho)}{2\rho}\,\delta(\tau), \ \text{ since } \int\delta(\hat{\mathbf{r}})d\mathbf{r} = 1. \tag{9}$$

Boundary conditions are easy to derive due to cylindrical symmetry of the solution (5). At the centre:

$$\left.\frac{\partial e}{\partial\rho}\right|_{\rho=0} = 0. \tag{10}$$

At outer surface, Ampere's law requires:

$$RH_{\varphi}(r=R) = \int_0^R J_z(r,t)rdr, \tag{11}$$

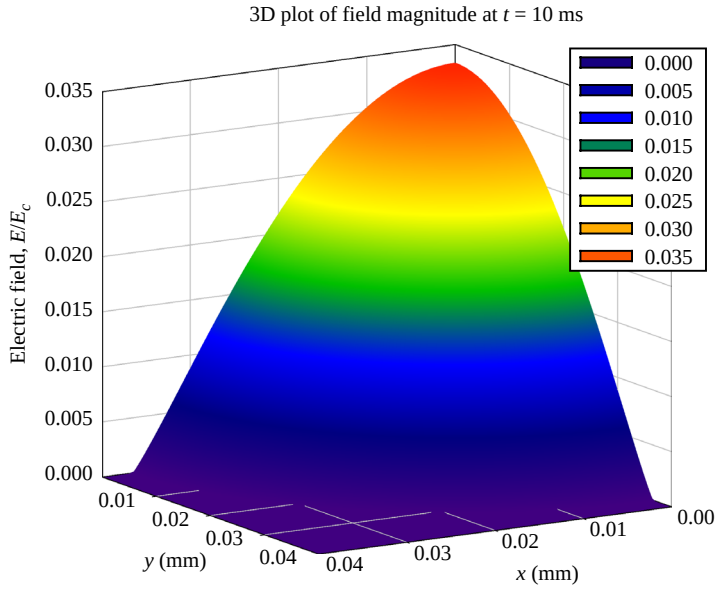

(a)

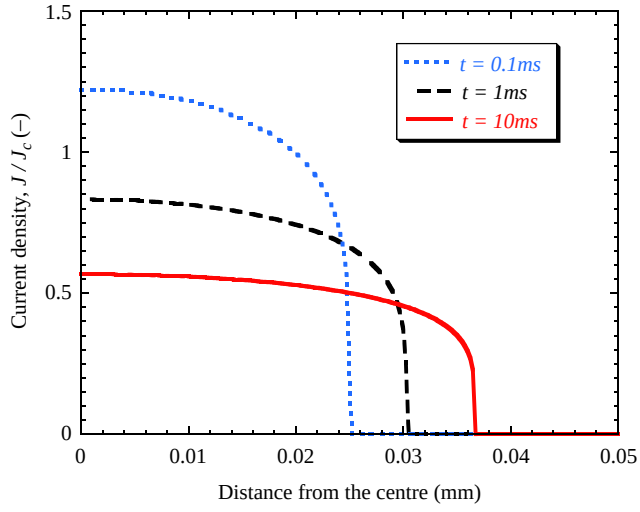

(b)

Notes: The exact solution is available for specific initial conditions given by equation (4); the analytical prediction of electric field and current density for a wire with I_0 = 2A, R = 0.5mm and α = 6 is shown at different instances of time; (a) electric field $E_z(x, y, t$ =10 ms); (b) current density $J_z(r, t)$

Figure 1.
Evolution of electric field and current density in a HTS wire of circular cross-section

which, after substituting into Faraday's law and applying dimensionless variables, results in:

$$\left.\frac{\partial e}{\partial \rho}\right|_{\rho=1} = \frac{\partial}{\partial \tau}\left(\int_0^1 i(\rho,\tau)\rho d\rho\right). \tag{12}$$

Combining equations (8) and (9) or, indeed, direct integration of equation (5) gives:

$$\left(\int_0^1 i(\rho,\tau)\rho d\rho\right) = \left(\int_0^{\rho_b} i(\rho,\tau)\rho d\rho\right) = \frac{i_0}{2} \equiv const. \tag{13}$$

According to equation (12), the boundary condition is:

$$\left.\frac{\partial e}{\partial \rho}\right|_{\rho=1} = 0, \tag{14}$$

which can be extended towards the front boundary:

$$\left.\frac{\partial e}{\partial \rho}\right|_{\rho=\rho_b} = 0, \quad e|_{\rho=\rho_b} = 0. \tag{15}$$

The additional boundary condition in equation (15) is in fact an implicit condition for the boundary ρ_b. Alternatively, it can be replaced by a conservation integral equation (13) as suggested in Golosnoy and Sykulski (2008). It is worth noting a discontinuity in the current density derivative at the boundary ρ_b:

$$\left.\frac{\partial i}{\partial \rho}\right|_{\rho=\rho_b-0} = \infty, \quad \left.\frac{\partial i}{\partial \rho}\right|_{\rho=\rho_b+0} = 0, \quad i|_{\rho=\rho_b} = 0. \tag{16}$$

The main objective of the study is to access a performance of various techniques on curved boundaries in multiple dimensions. This is why, despite the actual problem possessing cylindrical symmetry, further analysis is conducted in Cartesian coordinates. The curl operator in equation (3) may be written for the first quarter in Cartesian coordinates by taking account of equation (6) and the symmetry of the problem:

$$\frac{\partial}{\partial \tau}(\mathrm{sign} e \cdot |e|^{1/\alpha}) = \frac{\partial^2 e}{\partial x^2} + \frac{\partial^2 e}{\partial y^2}, \quad \rho^2 = x^2 + y^2, \quad x, y \in [0,1]. \tag{17}$$

It follows from equation (15) that appropriate boundary conditions for equation (17) would be:

$$\left.\frac{\partial e}{\partial x}\right|_{y=0} = 0, \quad \left.\frac{\partial e}{\partial y}\right|_{x=0} = 0, \tag{18}$$

at the symmetry lines and:

$$\frac{\partial e}{\partial \hat{\mathbf{n}}} = 0, \quad e = 0 \tag{19}$$

at any point behind the front edge ρ_b, with $\hat{\mathbf{n}}$ being the normal to the computational region boundary.

2.4 Conservation law

Pure Neumann boundary conditions (18) and (19) dictate a conservation integral:

$$\left(\int_0^1 \int_0^1 i(x,y,\tau)dxdy\right) = \frac{\pi i_0}{4} \equiv const. \tag{20}$$

3. Computational technique

3.1 Front-fixing method

Let us fix an extent of the computational region by some boundary $s(x,y) = 0$ as described in Crank (1984). In general, the transformed version of equation (17) contains mixed derivatives; this is not desirable for modelling of diffusion processes with sharp gradients since small time steps are required to suppress non-monotonic oscillations in the numerical solution (see Thomas (1999) and Tannehill *et al.* (1997) for general theory of monotonic solutions). Fortunately, the boundary condition (19) is an implicit one and may be imposed at any point behind the real boundary. It is convenient therefore to consider a rectangular region with moving edges $x_s(\tau)$, $y_s(\tau)$. An introduction of new variables $u = x/x_s$, $v = y/y_s$ fixes the extent of the computational domain to $0 \le u, v \le 1$. In order to derive a finite volume scheme, we have to integrate equation (17) over time and space intervals (LeVeque, 2002). The space is discretised at $M + 1$ points for u and at $K + 1$ points for v. The discretisation points are defined by a fixed discretisation of u, v and they are written as $u_0 = 0$, $u_1, \ldots, u_M = 1$, $v_0 = 0$, $v_1, \ldots, v_K = 1$. The finite volume discretisation (LeVeque, 2002) of equation (17) is based on integration around the nodes and is fairly straightforward (Illingworth and Golosnoy, 2005; Illingworth *et al.*, 2005), e.g. for the node (m, k), it may be written as:

$$\begin{aligned}
&(u_{m+0.5} - u_{m-0.5})(v_{k+0.5} - v_{k-0.5}) \int_{\tau^n}^{\tau^{n+1}} x_s y_s \cdot i_{m,k} d\tau \\
&= (v_{k+0.5} - v_{k-0.5}) \int_{\tau^n}^{\tau^{n+1}} y_s \left[\frac{1}{x_s}\frac{\partial e}{\partial u} + u\frac{dx_s}{dt}\cdot i\right]_{m-0.5,k}^{m+0.5,k} d\tau \\
&+ (u_{m+0.5} - u_{m-0.5}) \int_{\tau^n}^{\tau^{n+1}} x_s \left[\frac{1}{y_s}\frac{\partial e}{\partial v} + v\frac{dy_s}{dt}\cdot i\right]_{m,k-0.5}^{m,k+0.5} d\tau
\end{aligned} \tag{21}$$

The boundary conditions (18) and (19) appear naturally in equation (21):

$$\left.\frac{\partial e}{\partial u}\right|_{v=0} = 0, \quad \left.\frac{\partial e}{\partial v}\right|_{u=0} = 0 \text{ and } \left.\frac{\partial e}{\partial u}\right|_{v=1} = 0, \quad i|_{v=1} = 0, \quad \left.\frac{\partial e}{\partial v}\right|_{u=1} = 0, \quad i|_{u=1} = 0. \tag{22}$$

The finite volume discretisation for equation (22) immediately follows from the general form (equation (21)) and is straightforward (Rappaz *et al.*, 2003).

Comment. The cylindrically symmetric problem (8) with boundary conditions (14) and (15) can be discretised in a similar way as shown in Illingworth and Golosnoy (2005).

3.2 Numerical scheme

To develop unconditionally monotonic scheme, we restrict the consideration by combining an explicit method with an appropriate limiter (Thomas, 1999; Tannehill *et al.*, 1997) for the advection part in equation (21) with a fully implicit method for diffusion fluxes. The integrals over time in equation (21) result in an operator finite volume form with the advection fluxes split in the u- and v-directions:

$$U(p^{n+1} - p^n) = LA_u p^n + LA_v p^n + D_u e^{n+1} + D_v e^{n+1}, \tag{23}$$

$$p^n_{m,k} = (u_{m+0.5} - u_{m-0.5})(v_{k+0.5} - v_{k-0.5}) y^n_s x^n_s i^n_{m,k}, \quad e^n_{m,k} = \left(i^n_{m,k}\right)^{\alpha}, \tag{24}$$

$$A_u p^n_{m,k} = \frac{1}{(u_{m+0.5} - u_{m-0.5})} \frac{\left(x^{n+1}_s - x^n_s\right)}{x^{n+0.5}_s} \left(u_{m+0.5} p^n_{m+0.5,k} - u_{m-0.5} p^n_{m-0.5,k}\right), \tag{25}$$

$$A_v p^n_{m,k} = \frac{1}{(v_{k+0.5} - v_{k-0.5})} \frac{\left(y^{n+1}_s - y^n_s\right)}{y^{n+0.5}_s} \left(v_{k+0.5} p^n_{m,k+0.5} - v_{k-0.5} p^n_{m,k-0.5}\right), \tag{26}$$

$$D_u e^{n+1}_{m,k} = (\tau^{n+1} - \tau^n)(v_{k+0.5} - v_{k-0.5}) \frac{y^{n+1}_s}{x^{n+1}_s} \left(\frac{e^{n+1}_{m+1,k} - e^{n+1}_{m,k}}{u_{m+1} - u_m} - \frac{e^{n+1}_{m,k} - e^{n+1}_{m-1,k}}{u_m - u_{m-1}}\right), \tag{27}$$

$$D_v e^{n+1}_{m,k} = (\tau^{n+1} - \tau^n)(u_{m+0.5} - u_{m-0.5}) \times \frac{x^{n+1}_s}{y^{n+1}_s} \left(\frac{e^{n+1}_{m,k+1} - e^{n+1}_{m,k}}{v_{k+1} - v_k} - \frac{e^{n+1}_{m,k} - e^{n+1}_{m,k-1}}{v_k - v_{k-1}}\right), \tag{28}$$

where U is a unity operator and L is a limiter (Tannehill *et al.*, 1997; Thomas, 1999). The limiter L is chosen to be a linear combination of standard upwind/downwind with high-resolution schemes (25) and (26) (Thomas, 1999). Tests on one-dimensional cylindrically symmetric problems (LeVeque, 2002; Tannehill *et al.*, 1997; Thomas, 1999) indicate that appropriate choice of L could provide second-order accuracy in space. An introduction of p in equation (23) is due to the fact that the value of p is actually conserved during the coordinate transformation and diffusion. Additional equations to predict variations of x_s, y_s with time should be added to equation (23) as discussed in the implementation section.

3.3 Fractional steps

The numerical solution of equation (23) could be optimised, since:

(1) the application of A_u and A_v together results in strict stability conditions; and

(2) D_u, D_v are non-linear with broad spectra and the choice of iteration parameters for standard methods, e.g. Gauss-Seidel, is not obvious.

Both complications can be overcome by applying the so-called "fractional step" method, which replaces a sum on the left-hand side of equation (23) by a linked chain of one-dimensional equations:

$$U(p^{n+0.25} - p^n) = LA_u p^n, \tag{29}$$

$$U(p^{n+0.5} - p^{n+0.25}) = LA_v p^{n+0.25}, \tag{30}$$

$$U(p^{n+0.75} - p^{n+0.5}) = D_u e^{n+0.75}, \tag{31}$$

$$U(p^{n+1} - p^{n+0.75}) = D_v e^{n+1}. \tag{32}$$

It was found that strong non-linearity of the diffusion operator introduces large errors (Figure 2) which can be significantly reduced by introducing a symmetric sequence:

$$U((p_*)^{n+0.75} - p^{n+0.5}) = D_u (e_*)^{n+0.75}, \tag{33}$$

$$U((p_*)^{n+1} - (p_*)^{n+0.75}) = D_v (e_*)^{n+1}, \tag{34}$$

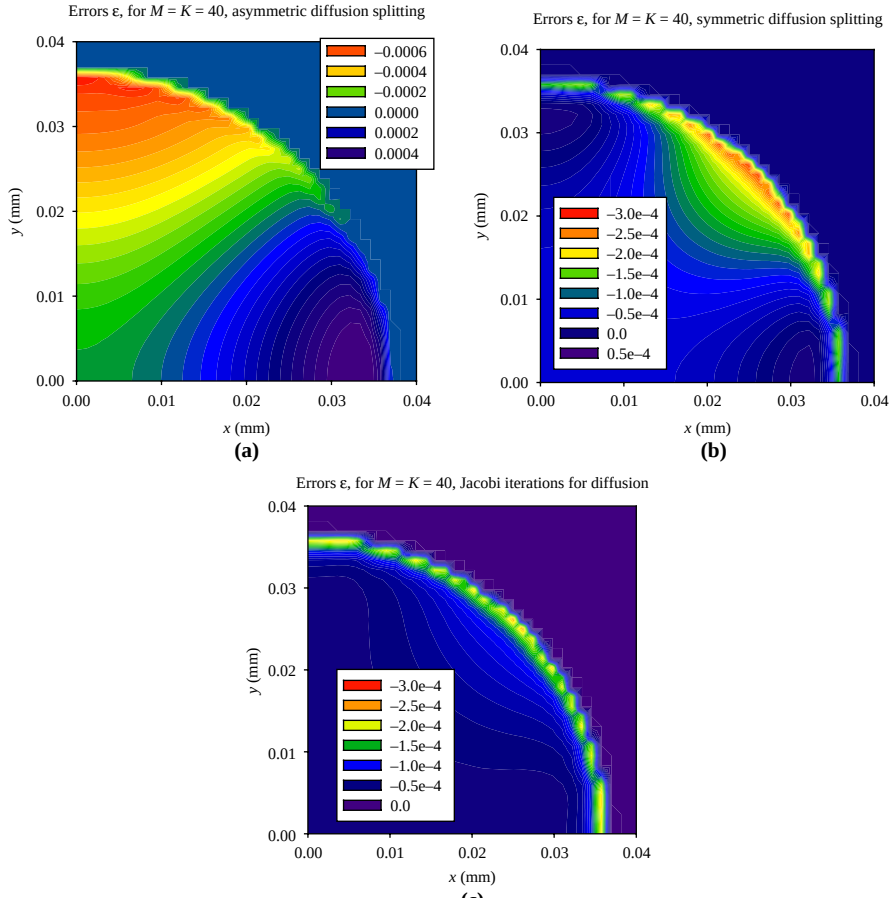

Figure 2.
Errors in predictions of electric field inside a HTS wire with $I_0 = 2\,\mathrm{A}$, $R = 0.5\,\mathrm{mm}$ and $\alpha = 6$ after $t = 10\,\mathrm{ms}$

Notes: A constant time step $\delta\tau = 10^{-6}$ s and a grid with $M = K = 40$ were used for predictions; (a) asymmetric form of diffusion split equation (31), equation (32) distorts the front shape: it becomes an ellipsoid extended in *x*-direction; (b) symmetrisation equations (33)-(37) decrease the errors and shifts them to $x = y$ plane; (c) coupled *u*-*v* scheme equation (38) with Jacobi iterations produce minimal errors but is very demanding in terms of computational time

$$U((p_{**})^{n+0.75} - p^{n+0.5}) = D_v(e_{**})^{n+0.75}, \tag{35}$$

$$U((p_{**})^{n+1} - (p_{**})^{n+0.75}) = D_u(e_{**})^{n+1}, \tag{36}$$

$$p^{n+1} = 0.5((p_{**})^{n+1} + (p_*)^{n+1}). \tag{37}$$

The solution of diffusion equations, e.g. equation (31), has been described in Golosnoy and Sykulski (2008). The proposed method equations (29), (30) and (33)-(37) requires only $O(MK)$ operations and is quite efficient. Another possible approach is to use Jacobi iterations (Tannehill *et al.*, 1997; Thomas, 1999) to solve:

$$U(p^{n+1} - p^{n+0.5}) = D_u e^{n+1} + D_v e^{n+1}, \tag{38}$$

linked with equations (29) and (30). Equation (38) should be solved simultaneously in both u and v directions. The symmetry is preserved by equation (38), but Jacobi iterations require $O(M^2K^2)$ operations and are inefficient for fine grids.

3.4 Implementation

Ideally, the edge of the computational region should coincide with the front boundary. But strong non-linear variations of field e or current i at the front prohibit the usage of any standard interpolations for the boundary equation (19) since this provides reasonable accuracy only for smooth solutions. A one-dimensional problem can replace the Neumann boundary condition with a conservation integral equation (13) (Golosnoy and Sykulski, 2008), but this is not feasible for a multidimensional case (equation (20)). Fortunately, we can extend slightly the computational domain, so that a few grid points stay in a zero field region. The algorithm iterates to choose $x_s(\tau^{n+1})$, $y_s(\tau^{n+1})$ in such a way that:

$$e^{n+1}_{M,k} = \varepsilon_1 > 0, \;\; k = 0, \ldots, K; \quad e^{n+1}_{m,K} = \varepsilon_1 > 0, \;\; m = 0, \ldots, M, \tag{39}$$

to enforce the zero field and:

$$e^{n+1}_{M-1,k} \le \varepsilon_2, \;\; k = 0, \ldots, K; \quad e^{n+1}_{m,K-1} \le \varepsilon_2, \;\; m = 0, \ldots, M, \tag{40}$$

to ensure negligible flux at the boundary. For a stable algorithm, $\varepsilon_1 = 10^{-300}$ was used and sufficient accuracy was achieved with $\varepsilon_2 = 10^{-100}$.

Careful examination of advection operators (25) and (26) reveal that the Courant number is usually greater than one, especially for initial stages of a pulse event when x_s, y_s are small. This is mainly due to large multiples $u/\Delta u \sim M$ and $v/\Delta v \sim K$ on the left-hand side of equation (25) or (26). The Courant-Friedrich-Levy condition (Tannehill *et al.*, 1997; Thomas, 1999) is not satisfied and explicit methods (25) and (26) are unstable. One possible way to overcome the problem is to move towards implicit methods. A standard upwind/downwind first-order scheme would introduce a large artificial diffusion at the front and is thus absolutely unsuitable, since the existence of the front is due to very sharp changes in diffusion fluxes themselves. Hence, high-order advection schemes with limiters have to be applied. Unfortunately, the only limiter which provides stable solution for a large Courant number is the "minmod" one (Tannehill *et al.*, 1997). However, tests suggest that this limiter provides only a small

improvement in comparison with an upwind/downwind scheme and its usage is not desirable.

To reduce the Courant number, the motion of the boundaries was split into additional h fractional steps. For each sub-step, $g = 0, \ldots, h-1$ a one-dimensional advection problem was solved:

$$U(p^{n+(g+1)/h} - p^{n+g/h}) = LA_u p^{n+g/h}, \tag{41}$$

with a small displacement $(x_s^{n+(g+1)/h} - x_s^{n+g/h})$ and explicit advection operator:

$$A_u p_{m,k}^{n+g/h} = \frac{1}{(u_{m+0.5} - u_{m-0.5})} \frac{\left(x_s^{n+(g+1)/h} - x_s^{n+g/h}\right)}{x_s^{n+0.5}} \left(u_{m+0.5} p_{m+0.5,k}^{n+g/h} - u_{m-0.5} p_{m-0.5,k}^{n+g/h}\right). \tag{42}$$

The number of displacements in equation (41) was chosen to keep the Courant number below unity.

A choice for limiter L was studied in details. A flux transport corrected SHASTA method (Boris and Book, 1976) was implemented together with "minmod" (Thomas, 1999), van Leer (van Leer, 1974), Sweby (Sweby, 1984), and "SuperBee" (Roe, 1986) limiters. It was found that the smallest numerical dissipation was given by the "SuperBee" (Roe, 1986) limiter. Therefore, this limiter was used for further tests.

3.5 Pulse event

A very high gradient of the electric field originates during the impulse of current. It spreads very quickly in all directions. Any attempt to use directional splitting equations (31) and (32), or even the symmetrical forms (33)-(37), results in unrealistically fast motion of the front. The problem can be solved by separating a pulse into sub-pulses with a smaller current input during individual sub-pulses (similar to what was done for advection operator A). To achieve good accuracy the number of sub-pulses in the first time step was found to be $\sim 10MK$ which makes the algorithm too slow. If alternatively Jacobi iterations are applied to the pulse event only (single time step), no introduction of sub-pulses is required. Further calculation can be carried on with directional splitting.

4. Results and discussion

Predictions from fixed grid calculations and the front-fixing method are shown in Figure 3. Variation of errors with an increasing number of space intervals $M = K$ are shown in Figure 3(a). The error ε is taken in a continuous $\mathbf{C}$ norm:

$$\varepsilon = \max_{m,k=0}^{M,K} \left| e_{m,k}^{\text{analytical}} - e_{m,k}^{\text{model}} \right| \tag{43}$$

A slope of the $M^{-1} - \varepsilon$ curve in log-log scale indicates only the first-order space approximation. This is true for both fixed grid and front-fixing approaches and is not affected by diffusion split introduced in equations (33)-(37). The asymmetric technique (29), equation (30) has a large directional bias (Figure 2(a)). The bias cannot be eliminated by mesh refinement and errors start to saturate at relatively high level. A symmetric version of the diffusion split equations (33)-(37) has almost the same

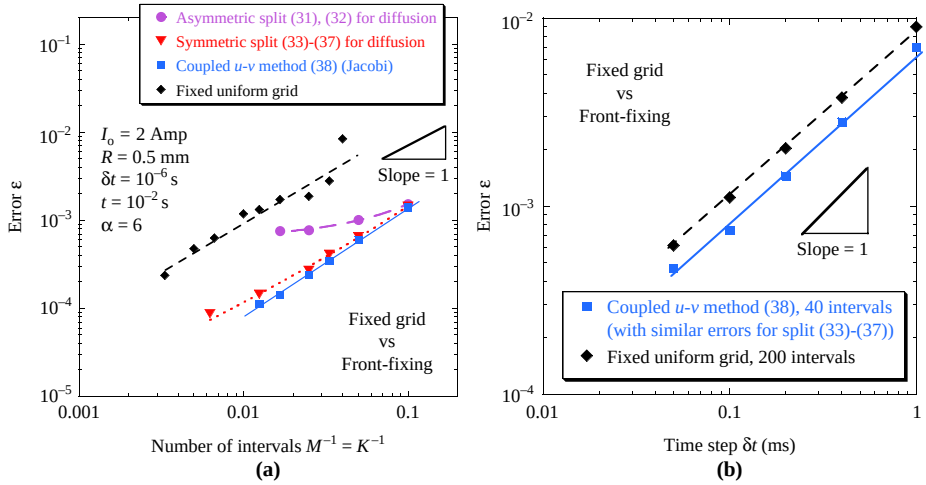

Figure 3.
Numerical prediction of an electric field $E_z(x, y)$ for a wire with $I_0 = 2$ A, $R = 0.5$ mm and $\alpha = 6$ after $t = 10$ ms

Notes: The mesh size and time step effects; (a) errors in predictions of an electric field at t = 0.01 s (small time step 1 μs) reveals an approximately first order of accuracy $O(M^{-1})$; (b) effect of time step on the errors (large number of grid points $M = K$); the results indicate that the algorithm has first-order accuracy in time $O(\delta\tau)$

accuracy as Jacobi method but requires significantly less computational effort. In fact, the symmetric split still has a directional bias which is an inherent feature of any split technique (Thomas, 1999); it is just moved to the $x = y$ plane (Figure 2(b)). Even the totally symmetric Jacobi method (38) has a slight bias around the $x = y$ plane, Figure 2(c), although it is hardly noticeable. The low-spatial accuracy in the continuous norm is a result of the sharp front with infinite derivatives in the solution. Since the errors concentrate around the front (Figure 3), then a convergence in any integral norm, e.g. $\boldsymbol{L}_1$, would be better. On the other hand, for the strongly coupled problems, the convergence in the $\mathbf{C}$ norm is of main importance.

Errors due to time discretisation were studied by varying δt between 0.05 and 1 ms for a large number of space intervals $M = K$. A combination of explicit advection with fully implicit diffusion approach provides a first-order approximation in time $O(\delta t)$ (Figure 3(b)). Such choice is dictated by high-field (current) gradients in the pulse event. When the pulse disperses slightly, it is possible to move towards the semi-implicit method with $O(\delta t^2)$ (Golosnoy and Sykulski, 2008) by applying Crank-Nicolson approximations for advection and diffusion operators in equations (25)-(28). The method can be improved further by the Lax-Wendroff explicit approach with limiters for equations (25) and (26) (Tannehill *et al.*, 1997; Thomas, 1999) and by the alternating direction implicit scheme for equations (27) and (28) (Tannehill *et al.*, 1997; Thomas, 1999). The latter should make the method approximately symmetric with reduced directional bias. (A small asymmetry will remain due to the application of the implicit scheme in one direction and the explicit one in the other.)

5. Conclusions

There are several advantages of using a front-fixing method for modelling of impulse phenomena in HTS, in particular high accuracy can be obtained with a small number

of grid points and large time increments. Moreover, standard numerical methods for convection problems with diffusion can be utilised in the front-fixing method. The following general observations can be made:

- Approximately, first order of spatial accuracy was found for all methods (stationary or mobile grids) for 2D problems with impulse events. Nevertheless, errors in the front-fixing technique are much smaller in comparison with fixed grids.
- Fractional steps method is proved to be an effective algorithm for solving the equations obtained. A symmetrisation procedure has to be introduced to eliminate a directional bias for standard asymmetric split of diffusion processes.

Practical considerations suggest that the following properties of the solution need to be noted and handled carefully:

(1) Complex boundary conditions have to be implemented by considering the conservation laws.

(2) A careful choice of a limiter for advection problems associated with the mesh motion needs to be made.

(3) Fully implicit schemes may be needed for pulse events, which limits the temporal accuracy. It is suggested to switch towards semi-implicit methods after the pulse disperses.

References

Berger, K., LeVeque, J., Netter, D., Douine, B. and Rezzoug, A. (2005), "AC transport losses calculation in a Bi-2223 current lead using thermal coupling with an analytical formula", *IEEE Transactions on Applied Superconductivity*, Vol. 15 No. 2, pp. 1508-11.

Boris, J.P. and Book, D.L. (1976), "Flux-corrected transport. III. Minimal-error FCT algorithms", *Journal of Computational Physics*, Vol. 20, pp. 397-431.

Crank, J. (1984), *Free and Moving Boundary Problems*, Clarendon Press, Oxford.

Golosnoy, I.O. and Sykulski, J.K. (2008), "Evaluation of the front-fixing method capabilities for numerical modelling of field diffusion in high-temperature superconducting tapes", *IET Science, Measurement & Technology*, Vol. 2 No. 6, pp. 418-26.

Illingworth, T.C. and Golosnoy, I.O. (2005), "Numerical solutions of diffusion-controlled moving boundary problems which conserve solute", *Journal of Computational Physics*, Vol. 209 No. 1, pp. 207-25.

Illingworth, T.C., Golosnoy, I.O., Gergely, V. and Clyne, T.W. (2005), "Numerical modelling of transient liquid phase bonding and other diffusion controlled phase changes", *J. Mater. Sci.*, Vol. 40 Nos 9/10, pp. 2505-11.

LeVeque, R.J. (2002), *Finite Volume Methods for Hyperbolic Problems*, Cambridge University Press, Cambridge.

Pert, G.J. (1977), "A class of similar solutions of the non-linear diffusion equation", *J. Phys. A: Math. Gen.*, Vol. 10 No. 4, pp. 583-93.

Rappaz, M., Bellet, M. and Deville, M. (2003), *Numerical Modeling in Materials Science and Engineering*, Springer, Berlin.

Rhyner, J. (1993), "Magnetic properties and AC-losses of superconductors with power law current-voltage characteristics", *Physica C*, Vol. 212, pp. 292-300.

Roe, P.L. (1986), "Characteristic-based schemes for the Euler equations", *Ann. Rev. Fluid Mech.*, Vol. 18, pp. 337-65.

Sweby, P.K. (1984), "High resolution schemes using flux-limiters for hyperbolic conservation laws", *SIAM J. Num. Anal.*, Vol. 21, pp. 995-1011.

Sykulski, J.K., Stoll, R.L. and Mahdi, A.E. (1997), "Modelling HTc superconductors for AC power loss estimation", *IEEE Transactions on Magnetics*, Vol. 33 No. 2, pp. 1568-71.

Tannehill, J.C., Anderson, D.A. and Pletcher, R.H. (1997), *Computational Fluid Mechanics and Heat Transfer*, Taylor & Francis, London.

Thomas, J.W. (1999), *Numerical Partial Differential Equations: Conservation Laws and Elliptic Equations*, Springer, New York, NY.

van Leer, B. (1974), "Towards the ultimate conservative difference scheme II. Monotonicity and conservation combined in a second order scheme", *Journal of Computational Physics*, Vol. 14, pp. 361-70.

About the authors

I.O. Golosnoy received his MSc degree in Applied Mathematics and Physics from the Moscow Institute of Physics and Technology, Russia in 1992 and the PhD in Mathematics and Physics from the Institute for Mathematical Modelling, Moscow, Russia. He is currently a Lecturer at the Electrical Power Engineering Group, School of Electronics and Computer Science, University of Southampton. His research interests include numerical modelling of various coupled electrical, thermal and mechanical phenomena with emphasis on free and moving boundaries problems. I.O. Golosnoy is the corresponding author and can be contacted at: ig@ecs.soton.ac.uk

J.K. Sykulski is a Professor of Applied Electromagnetics at the University of Southampton. His research interests are in the areas of power applications of high-temperature superconductivity, modelling of superconducting materials, advances in simulation of coupled field systems (electromagnetic, circuits and motion), development of fundamental methods of computational electromagnetics and new concepts in design and optimisation of electromechanical devices. He has over 300 publications listed on the official database of the university. He is a Founding Member and a Chair of the Professional Network Electromagnetics of the IET, a Founding Secretary/Treasurer/Editor of the International Compumag Society, a Visiting Professor at universities in Canada, France, Italy, Poland and China and a Member of International Steering Committees of major international conferences, including COMPUMAG, IEEE CEFC, IEE CEM, EMF, ISEF, EPNC, ICEF and others. He is a Fellow of IEEE, IET, Institute of Physics and British Computer Society and has an honorary title of Professor awarded by the President of Poland.